

Substantial loss of isoprene in the surface ocean due to chemical and biological consumption

Rafel Simó ¹✉, Pau Cortés-Greus¹, Pablo Rodríguez-Ros¹ & Marta Masdeu-Navarro¹

Isoprene contributes to the formation of ozone and secondary organic aerosol in the atmosphere, and thus influences cloud albedo and climate. Isoprene is ubiquitous in the surface open ocean where it is produced by phytoplankton, however emissions from the global ocean are poorly constrained, in part due to a lack of knowledge of oceanic sink or degradation terms. Here, we present analyses of ship-based seawater incubation experiments with samples from the Mediterranean, Atlantic, tropical Pacific and circum-Antarctic and Subantarctic oceans to determine chemical and biological isoprene consumption in the surface ocean. We find the total isoprene loss to be comprised of a constant chemical loss rate of $0.05 \pm 0.01 \text{ d}^{-1}$ and a biological consumption rate that varied between 0 and 0.59 d^{-1} (median 0.03 d^{-1}) and was correlated with chlorophyll-a concentration. We suggest that isoprene consumption rates in the surface ocean are of similar magnitude or greater than ventilation rates to the atmosphere, especially in chlorophyll-a rich waters.

¹Institut de Ciències del Mar, ICM-CSIC, Barcelona, Catalonia, Spain. ✉email: rsimo@icm.csic.es

Isoprene (2-methyl-1,3-butadiene) emissions by terrestrial and marine life are altogether of a magnitude similar to the sum of natural and anthropogenic emissions of methane^{1,2}, ca. 500 TgC year⁻¹. Owing to its reactivity and short lifetime in the atmosphere³ (minutes to hours), isoprene impacts atmospheric chemistry by forming tropospheric ozone, modifying the oxidation behaviour of other organic compounds, and contributing to secondary organic aerosols^{4,5}. Even though the oceans emit much less isoprene than vegetated land, the potential of biogenic aerosols to influence cloud albedo and lifetimes, hence climate, is large over the vast oceans remote from anthropogenic sources⁶.

On land, isoprene is produced and released mainly by trees and shrubs⁷. In the ocean, isoprene is produced primarily by phytoplankton⁸ and also by seaweeds⁹. Whilst in vascular plants isoprene production is related to rapid alleviation of thermal and oxidative stress and chemical signalling^{10,11}, the ecophysiological functions of isoprene biosynthesis in phytoplankton are unknown, yet a similar antioxidant role has been speculated¹². In any case, isoprene is ubiquitous in the surface ocean, where it occurs at concentrations mostly within the 1–100 nmol m⁻³ range^{13,14}.

Estimations of the global ocean emission of isoprene have been attempted either by top-down (balancing modelled emissions to atmospheric observations) or bottom-up (modelling oceanic isoprene concentration and air–sea flux) approaches, and they diverge by one or two orders of magnitude¹⁴ (maximum range: 0.1–12 TgC year⁻¹). In general, top-down estimates are much higher, which implies that atmospheric measurements, as well as knowledge of the atmospheric processes, are insufficient to properly constrain the top-down models, and/or the bottom-up studies underestimate the net isoprene production. An extra isoprene source through photoproduction by surfactants in the sea surface microlayer was invoked and experimentally demonstrated¹⁵ but later esteemed not enough to resolve the large discrepancy¹⁶. In any case, the difficulties in constraining the global marine isoprene emission have evidenced that knowledge of the magnitude, drivers, distribution, and dynamics of isoprene cycling processes is still poor due to lack of measurements and depends too much on a number of assumptions and laboratory-based studies^{11,14,17}.

It is thought that not all the isoprene produced by phytoplankton escapes to the atmosphere because part of it is degraded in seawater, but the actual proportion is unknown. Chemical oxidation is taken for granted¹⁸ because of isoprene's high

reactivity¹⁹, but it has never been measured. Likewise, the occurrence of isoprene-degrading bacteria in seawater has been demonstrated^{20,21} and a significant microbial sink has been suggested^{22–24}, but it has not been experimentally confirmed, let alone measured, in natural conditions including natural concentrations.

We conducted seawater incubations with the aim to determine if isoprene was chemically and biologically consumed in the surface ocean. Detailed time courses with coastal seawater informed on the kinetics of isoprene loss, and these kinetics were used to calculate loss rates from incubations conducted during four oceanographic expeditions across the Mediterranean Sea and the Atlantic Ocean, in the Tropical Pacific, and in Antarctic and Subantarctic waters. The obtained loss rate constants were compared with rate constants of air–sea flux and vertical mixing, and their variability across samples was examined by comparison with biological and environmental variables, with the aim to propose a predictive model that fills a major gap in the assessment of isoprene turnover in the surface ocean.

Results and discussion

Evidence for biological and chemical isoprene consumption in coastal seawater. The time course of isoprene concentration in coastal seawater samples incubated in closed glass bottles at the in situ temperature and in the dark demonstrated sustained loss for at least 45 h (Fig. 1a). Enclosure without headspace prevented isoprene loss by ventilation, and darkness was assumed to arrest all or most of the biological production²⁵ and any photochemical production¹⁵ or degradation. Thus, the measured loss was considered the result of microbial degradation and chemical oxidation. In most cases an exponential function fitted better the decay than a linear function (Supplementary Table 1), indicating first-order (concentration-dependent) kinetics for isoprene loss.

Incubation of microorganism-devoid (filtered through 0.2 μm) coastal seawater sampled next to seaweeds showed an isoprene loss (0.12 d⁻¹) that was half the loss in non-filtered water (0.20 d⁻¹; Fig. 1b and Supplementary Table 2), implying that chemical oxidation accounted for half the total loss. Oxidation by OH·, the fastest amongst isoprene reactions with oxidative transients for which reaction rate data exist¹⁹, could account for the observed chemical loss. However, the possibility of oxidation by hitherto overlooked, pervasive oxidants like H₂O₂ deserved consideration. The addition of unrealistically high concentrations of either H₂O₂

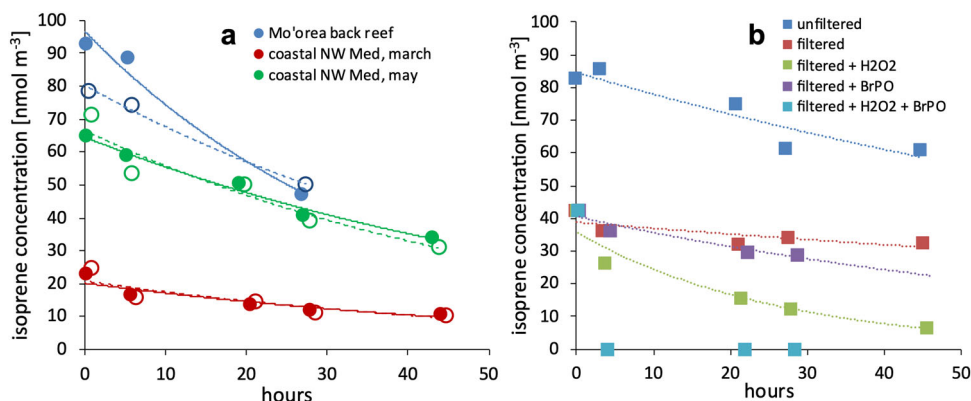


Fig. 1 Isoprene loss in dark incubations of coastal seawater. **a** Time course of isoprene concentration in 2 L dark incubations of non-filtered seawater samples from the back-reef lagoon of Mo'orea in April (blue) and the coastal Mediterranean in March (red) and May (green). Filled and open symbols correspond to duplicate incubations. Exponential fits to the data are shown by lines. See Supplementary Table 1 for fit equations and metrics, water temperatures and chlorophyll *a* concentrations. **b** Time course of isoprene concentration in series of 30 mL dark incubations of coastal Mediterranean seawater. Dark blue: non-filtered; red: filtered through 0.2 μm; green: filtered + 10 μmol L⁻¹ H₂O₂; purple: filtered + 0.0025 units mL⁻¹ bromoperoxidase (BrPO); light blue: filtered + H₂O₂ + BrPO. Exponential fit results in Supplementary Table 2.

or the enzyme bromoperoxidase (BrPO), substantially speeded up the chemical loss (0.91 d^{-1} with $10 \mu\text{mol H}_2\text{O}_2 \text{ L}^{-1}$, 0.31 d^{-1} with $0.0025 \text{ units BrPO mL}^{-1}$; Fig. 1b and Supplementary Table 2). Isoprene could have reacted with H_2O_2 in seawater as it does in acidic aerosols²⁶. Besides, should dissolved²⁷ BrPOs from seaweeds or outer-membrane-bound²⁸ BrPOs from phytoplankton occur, they would have reacted with added H_2O_2 to produce hypobromous acid (HOBr), a strong oxidant²⁹ that would further remove isoprene. Indeed, the addition of BrPO consumed isoprene because it produced HOBr by reaction with the naturally occurring H_2O_2 . Confirming this interpretation, large HOBr production by simultaneous addition of BrPO and H_2O_2 caused complete isoprene removal in less than 4 h (Fig. 1b). Therefore, the results shown in Fig. 1b indicate that isoprene is reactive to pervasive H_2O_2 either directly or through the formation of enzymatically derived HOBr. All in all, first-order total isoprene loss (Fig. 1a) is expected to depend on photochemically-produced oxidants³⁰ like H_2O_2 , OH· and $^1\text{O}_2$ as well as on microbiota through (a) microbial uptake and catabolism¹¹ and (b) reaction with biologically produced oxidants^{26,31,32} like HOBr, H_2O_2 or superoxide.

Variability of isoprene loss rate constants in the open ocean.

Ten of the eleven offshore experimental sites were located in the open ocean, and one was located on the Southwestern Atlantic Shelf. Altogether they covered wide ranges of latitude (40°N – 61°S), sea surface temperature (-0.8 – 28.6°C), daily-averaged wind speed (3 – 12 m s^{-1}), fluorometric chlorophyll-*a* (*chl a*) concentration (0.1 – 5.8 mg m^{-3}), and isoprene concentration (4 – 104 nmol m^{-3}) (Fig. 2, Table 1 and Supplementary Table 3). Unfiltered seawater samples from the surface ocean were incubated in glass bottles for 24 h, at the in situ temperature and in the dark, and first-order loss rate constants were determined from initial and final isoprene concentrations (see Methods). Note that loss was determined under the assumption that isoprene production was arrested in the dark²⁵. There is published evidence that residual isoprene production may occur in the dark³³, but in our incubations, it was insufficient to counteract loss. Thus, isoprene losses caused by processes other than ventilation may have been underestimated.

Loss rate constants ($k_{\text{loss}} = k_{\text{bio}} + k_{\text{chem}}$) varied over an order of magnitude, ranging 0.03 – 0.64 d^{-1} with a median of 0.08 d^{-1} (Table 1). They did not show any significant relationship to sea surface temperature (SST) (Supplementary Fig. 1) but showed proportionality to the *chl a* concentration (Fig. 3a) that was best

described by the following linear regression equation:

$$k_{\text{loss}} = 0.10 (\pm 0.01) x [\text{chl}a] + 0.05 (\pm 0.01) \quad (1)$$

The fact that the variability of k_{loss} is largely driven by [*chl a*] suggests that the variable term ($0.10 \times [\text{chl}a]$) corresponds to microbiota-dependent consumption (k_{bio}), which in our experiments gave values between 0 and 0.59 d^{-1} , with a median of 0.03 d^{-1} . These are the first experimental estimates of their kind and, hence, there are no other data to compare to. With a lack of experimental data, a pioneering modelling study¹⁸ proposed the use of a fixed k_{bio} at 0.06 d^{-1} ; more recently²³, though, the need for a variable k_{bio} spanning at least between 0.01 and 0.1 d^{-1} was invoked to balance observed concentrations in situ with predictions of the production term from phytoplankton culture data once the ventilation and chemical losses were accounted for. Our experimental results indicate that such variable k_{bio} indeed exists and spans even a broader range. The most complete model of the global oceanic isoprene cycle to date¹⁷ also performed the best simulations with a variable k_{bio} . This was computed proportional to the simulated [*chl a*], with a proportionality coefficient of 0.054, i.e. roughly half the coefficient we obtained by linear regression of observations (0.10).

Part of the k_{bio} (or variable k_{loss}) is to be attributed to degradation or utilisation by heterotrophic bacteria. A pioneering study²⁰ demonstrated the potential for bacterial consumption after isoprene additions at concentrations at least four orders of magnitude higher than natural concentrations. This has been accompanied by sparse but solid evidence^{20,21,34} for the presence in marine waters of isoprene-degrading bacteria belonging mainly to the phylum *Actinobacteria*. Two more recent studies^{24,35} suggested that members of the ubiquitous SAR11, the most abundant bacterial clade in the ocean, can also consume isoprene, but this was mainly based on indirect evidence and requires confirmation. Our k_{loss} did not show any significant correlation with the total bacterial abundance (Table 1). It must be noted, though, that bacterial abundance does not necessarily parallel heterotrophic bacterial activity, less so the activity of specific phyla, whereas a general trend of higher bacterial activity with higher [*chl a*] is commonly observed³⁶. Besides, phytoplankton-derived oxidants like the aforementioned H_2O_2 and HOBr may have also contributed to the dependence of isoprene loss on [*chl a*]. Circumstantial evidence in one study³⁷ suggested that the cosmopolitan cyanobacterium *Synechococcus* might consume isoprene; it is worth noting that *Synechococcus* harbours membrane-bound BrPO³⁸ and may, thus, consume isoprene as a side-process of combatting oxidative stress caused by H_2O_2 . If confirmed, this could have contributed to the correlation between k_{loss} and [*chl a*]. However, the three highest k_{loss} of our experimental series were measured in waters colder than 14°C where *Synechococcus* occurred at very low biomass^{39,40}. Therefore, these cyanobacteria cannot be invoked as responsible for the high k_{loss} paralleling high [*chl a*], and a large proportion of the k_{bio} term of k_{loss} must correspond to degradation by heterotrophic bacteria³⁴ as well as to reaction with biogenic oxidants from phytoplankton.

We attribute the intercept of Eq. (1) to a less variable loss by microbiota-independent chemical oxidation¹⁸, k_{chem} . In remarkable support to this, the value of the intercept, $0.05 \pm 0.01 \text{ d}^{-1}$, coincides with the k_{chem} commonly prescribed in models hitherto^{17,18,41}, which was calculated from reaction rate constants and estimated steady-state concentrations of photochemically-produced OH· and $^1\text{O}_2$ in the surface ocean.

Despite the limited number of experiments, the fact that they cover a wide range of contrasting oceanic regions and conditions confers to Eq. (1) the potential to be used in numerical models of

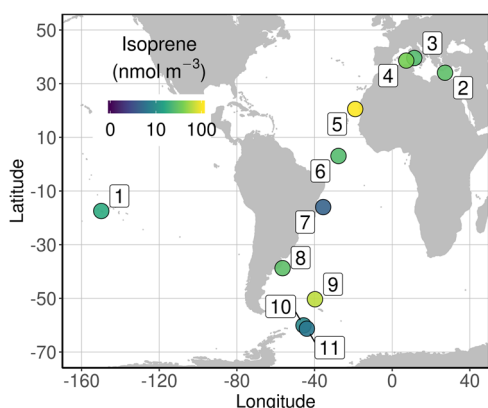


Fig. 2 Geographical distribution of the offshore experiments. Location of the sampling and incubation sites are shown by circles, coloured for isoprene concentration.

Table 1 Measured biological variables and isoprene process rate constants.

sample (# on map) ^a	SST (°C)	Chla (mg m ⁻³)	BA (10 ⁶ cell mL ⁻¹)	isoprene (nmol m ⁻³)	<i>k</i> _{loss} (d ⁻¹)	<i>k</i> _{vent} (d ⁻¹)	<i>k</i> _{mix} (d ⁻¹)	total τ (d)	<i>k</i> _{prod} (d ⁻¹)	sp. prod. rate (nmol (mg chla) ⁻¹ d ⁻¹)
Trop. Pacific										
1	28.6	0.31	0.92	17.5	0.06	0.03	-0.005 ^b	11.2	0.08	4.8
Mediterranean										
2	18.9	0.15	0.64	27.8	0.09	0.08	-0.005 ^b	6.0	0.16	29.9
3	19.1	0.19	0.86	25.1	0.07	0.10	-0.005 ^b	6.0	0.16	21.3
4	16.8	0.15	1.32	39.0	0.03	0.03	-0.005 ^b	15.5	0.06	15.8
Atlantic										
5	23.4	0.61	1.46	104.1	0.15	0.08	-0.005 ^b	4.4	0.22	37.9
6	28.1	0.20	1.29	25.0	0.04	0.07	-0.005 ^b	9.3	0.10	13.0
7	25.5	0.11	0.78	4.5	0.08	0.11	-0.005 ^b	5.4	0.18	7.3
8	13.9	1.67	2.64	27.6	0.28	0.16	-0.005 ^b	2.3	0.44	7.2
S. Ocean										
9	5.0	5.77	0.63	64.2	0.64	0.07	0.001	1.4	0.71	7.9
10	1.0	1.96	0.23	8.8	0.19	0.06	-0.005	4.0	0.25	1.1
11	-0.8	0.29	0.36	6.3	0.06	0.14	-0.010	4.9	0.19	4.2

SST sea surface temperature, chla chlorophyll-*a* concentration, BA bacterial abundance, *k*_{loss} rate constant of isoprene loss in incubations (microbial degradation + chemical oxidation), *k*_{vent} rate constant of isoprene ventilation to the atmosphere, *k*_{mix} rate constant of isoprene vertical mixing by turbulent diffusion at the bottom of the mixed layer (negative means import into the surface mixed layer), total τ turnover time due to all sinks, *k*_{prod} rate constant of isoprene production, assuming 24-h steady-state for the isoprene concentration, sp. prod. rate chla-normalised daily rate of isoprene production.

^aMap in Fig. 2; coordinates in Supplementary Table 2.

^bTaken from the global integral suggested by a model¹⁷.

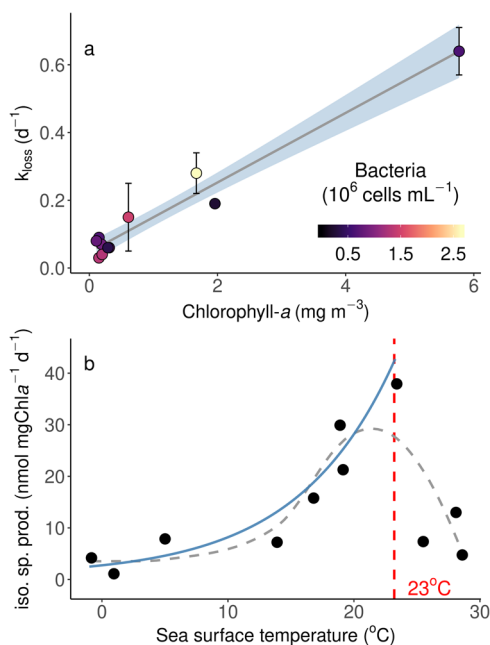


Fig. 3 Isoprene processes and their main drivers. **a** Rate constant of isoprene loss in dark incubations (*k*_{loss}, considered to be microbial and chemical consumption) vs. chlorophyll-*a* concentration. The linear regression equation is $k_{\text{loss}} = 0.10 \times [\text{chla}] + 0.05$ ($R^2 = 0.96$, $p = 10^{-7}$, $n = 11$). The standard error of the slope is $0.01 \text{ L mg}^{-1} \text{ d}^{-1}$, and the standard error of the intercept is 0.01 d^{-1} . Error bars represent the experimentally determined standard error of *k*_{loss}. The colour scale of the circles indicates bacterial abundances. **b** Specific (chla-normalised) rate of isoprene production vs seawater temperature (SST) across the sample series. The dashed line is the general smoothed trend. The blue line is the exponential adjustment at SST < 23 °C: $\text{iso. sp. prod.} = 2.04 \times e^{(0.13 \cdot \text{SST})} + 0.71$ ($R^2 = 0.85$, $p = 10^{-3}$, $n = 8$).

marine isoprene cycling, replacing the fixed term for microbial consumption^{18,41}. The *k*_{loss} vs. [chla] relationship here proposed can also be used to predict *k*_{loss} from remote sensing chla measurements (chla_{sat}). It must be noted, however, that the algorithms used to obtain [chla_{sat}] from satellite spectral data and

to compare among sensors, are validated against HPLC-measured chla⁴², not against the fluorometric chla that was used in Eq. (1). To convert fluorometric to satellite chla concentrations we used a relationship obtained with a global compilation of in situ fluorometric measurements and their match-ups from SeaWiFS and MODIS Aqua sensors:⁴³

$$[\text{chla}_{\text{sat}}] = 0.79 \times [\text{chla}]^{0.78} \quad (R^2 = 0.66, n > 1000) \quad (2)$$

Substitution in Eq. (1) results in:

$$k_{\text{loss}} = 0.14 \times [\text{chla}_{\text{sat}}]^{1.28} + 0.05 \quad (3)$$

which is our recommended equation for *k*_{loss} prediction from satellite chla. Note that only the variable term (*k*_{bio}) changes from Eq. (1), while the intercept (*k*_{chem}) is maintained at 0.05 d^{-1} .

Comparison of isoprene sinks and total turnover time. The change of isoprene concentration ([iso]) in the surface mixed layer over time can be described as the budget of sources and sinks:

$$\Delta[\text{iso}]/\Delta t = [\text{iso}] \cdot (k_{\text{prod}} - k_{\text{loss}} - k_{\text{vent}} - k_{\text{mix}}) \quad (4)$$

where *k*_{prod}, *k*_{vent} and *k*_{mix} are the rate constants of isoprene production, ventilation to the atmosphere and vertical downward mixing by turbulent diffusion, respectively.

We calculated *k*_{vent} from our sampling sites over a period of 24 h (Table 1). Ventilation has been considered the main isoprene sink from the upper mixed layer of the ocean¹⁸. In our sampling sites, *k*_{loss} was 0.4 to 10 times the *k*_{vent} (median factor: 1.2). That is, loss through microbial + chemical consumption was of the same order as ventilation, sometimes considerably faster. Vertical mixing, *k*_{mix}, was estimated to be one order of magnitude lower than the other process rates (Table 1), and in all cases but one it was calculated or assumed not to be a loss term but an import term into the mixed layer, because vertical profiles generally show maximum isoprene concentrations below the mixed layer and turbulent diffusion causes upward transport^{14,17}. Altogether, the microbial, chemical, ventilation, and, where relevant, mixing losses resulted in total turnover times ($1/(k_{\text{loss}} + k_{\text{vent}} + k_{\text{mix}})$) of isoprene between 1.4 and 16 days, median 5 days (Table 1).

Isoprene production. Assuming steady-state for isoprene concentrations over 24 h (Supplementary Fig. 2), i.e. $\Delta[\text{iso}]/\Delta t = 0$ in Eq. (4), the sum of the daily rate constants of all sinks ($k_{\text{loss}} + k_{\text{vent}}$) equals the rate constant of isoprene production (k_{prod}), with k_{mix} adding to either side depending on whether it is an import to or an export from the mixed layer (Table 1). Note that k_{prod} was the highest coinciding with higher $[\text{chl}a]$. This is consistent with a recent study⁴⁴ where measurement of the net biological isoprene production (i.e. production — consumption rates) across seasons in the open ocean was attempted; net production rates increased in May, coinciding with a large increase in $[\text{chl}a]$ and phytoplankton cell abundance.

The product of k_{prod} by the isoprene concentration gives the daily isoprene production rate, which can be normalised by dividing it by the $\text{chl}a$ concentration. In our study, this specific isoprene production rate varied between 1 and 38 $\text{nmol} (\text{mg chl}a)^{-1} \text{d}^{-1}$ (Table 1), median 8 $\text{nmol} (\text{mg chl}a)^{-1} \text{d}^{-1}$. These values are within the broad range reported across phytoplankton taxa from laboratory studies with monocultures^{41,45} (0.3–32, median 3 $\text{nmol} (\text{mg chl}a)^{-1} \text{d}^{-1}$, $n = 124$). Five of the eleven sites gave values $>13 \text{ nmol} (\text{mg chl}a)^{-1} \text{d}^{-1}$, i.e. in the higher end of the laboratory data range. This is not unexpected, since measurements in monoculture experiments are typically conducted before reaching nutrient limitation, below light saturation and in the absence of UV radiation, to mention three stressors commonly occurring in the surface open ocean. If isoprene biosynthesis and release is enhanced by any of these stressors, as is the case in vascular plants^{7,10}, then monoculture-derived results will easily render underestimates of isoprene production in the open ocean. Production by heterotrophic bacteria⁴⁶ could have also contributed to increase apparent specific isoprene production rates, but the occurrence and importance of this process in the marine environment is unknown.

When plotted against the SST, which was also the temperature of the incubations, specific isoprene production rates increased exponentially between -0.8 and 23°C and dropped drastically at higher SST (Fig. 3b). Several studies with phytoplankton monocultures have reported positive dependence of specific isoprene production rates on temperature^{45,47–50}. One of these studies⁴⁵ described that the increase with temperature reaches an optimum for production that varies among phytoplankton strains and with light intensity, but falls around $23\text{--}26^\circ\text{C}$. The most detailed study⁴⁷ was conducted with a *Prochlorococcus* strain;

remarkably, the shape of the specific production rate vs. temperature curve for this cyanobacterium strain was almost identical to that of Fig. 3b, with an exponential increase until 23°C and a drop thereafter. This is the canonical curve type of enzymatic activities, but the thermal behaviour of the enzymes for isoprene synthesis in marine unicellular algae has not yet been characterised¹².

Revising the magnitude and players of the marine isoprene cycle.

Our results allow redrawing the isoprene cycle in the surface mixed layer of the ocean. Figure 4 sketches the magnitude of the rate constants for production and sinks presented in Table 1, averaged according to a $\text{chl}a$ concentration threshold: the blue and green arrows correspond to the experiments in waters with $[\text{chl}a]$ lower and higher than 0.4 mg m^{-3} , respectively. Isoprene production in productive ($\text{chl}a$ -richer) waters is faster than in oligotrophic ($\text{chl}a$ -poorer) waters. Vertical mixing is assumed to majorly constitute an input into the mixed layer, yet very small. Photochemical production and emission from surfactants¹⁵ in the surface microlayer of productive waters is depicted as uncertain. Among sinks, the microbiota-dependent consumption is much faster in productive waters; actually, the statistical uncertainty of Eq. (1) and the uneven distribution of incubation results along the $[\text{chl}a]$ axis hamper resolving k_{bio} in phytoplankton-poor waters ($<0.4 \text{ mg m}^{-3}$), which represent nearly 80% of the area of the global surface ocean as a monthly average. Here, k_{loss} can be anything between 0.03 and 0.09 d^{-1} , and therefore k_{bio} will be $<0.04 \text{ d}^{-1}$. Putative purely chemical oxidation is considered invariant irrespective of the $\text{chl}a$ content; consequently, the combined microbial + chemical loss is much faster in productive waters. The k_{vent} for ventilation to the atmosphere is not significantly different between the two groups because it depends on wind speed and SST, which are both independent of $[\text{chl}a]$.

Note that this comparison applies to process rate constants k (d^{-1}), which represent the velocities at which processes occur and are attributable to biological and environmental agents. The actual process rates ($\text{nmol m}^{-3} \text{d}^{-1}$) will result from multiplying each of these k by the isoprene concentration, $[\text{iso}]$. Even though $[\text{iso}]$ tends to increase with $[\text{chl}a]$, there is no such a thing as a globally valid proportionality between the two^{13,14,51} (Table 1). All in all, more

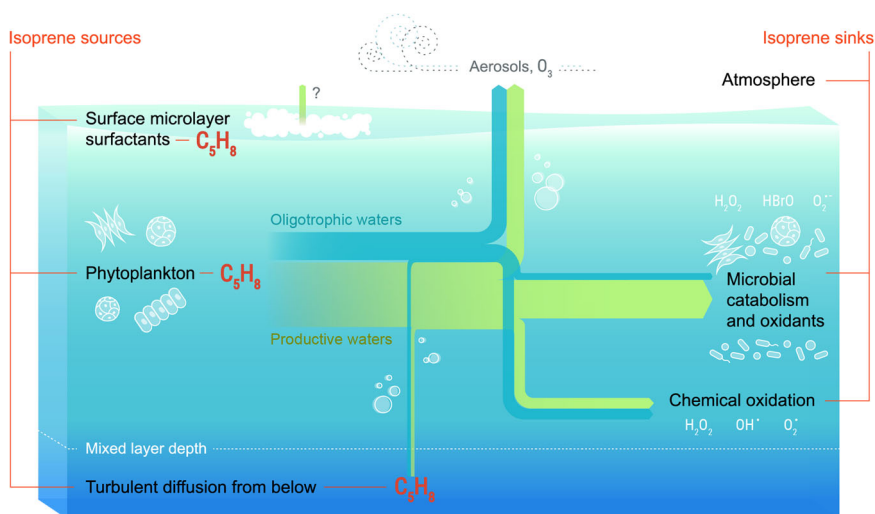


Fig. 4 Relative magnitude of isoprene cycling processes in the surface ocean, according to oceanic productivity. The width of the arrows is proportional to the magnitude of the process rate constants (d^{-1}), which have been averaged from the seven oligotrophic sites with $[\text{chl}a] < 0.4 \text{ mg m}^{-3}$ (blue arrows) and from the four productive sites with $[\text{chl}a] > 0.4 \text{ mg m}^{-3}$ (green arrows). Note the change in the relative magnitude of the sinks. The question mark next to the isoprene emission from photochemical reactions onto sea surface surfactants indicates the uncertainty in the magnitude of this source in productive waters.

isoprene is produced in productive waters but more is consumed as well; therefore, predicting the resulting effect on isoprene concentrations and air–sea fluxes is not straightforward.

Concluding remarks. Until now, most of the focus of isoprene cycling studies had been on the production term, considering specific production rates by phytoplankton as though they were constitutive and shaped by phylogeny⁴¹, with an occasional emphasis on how they are tuned by acclimation to environmental conditions^{45,47,50}. Even though teasing apart phylogeny and acclimation at the cross-basin and seasonal scales is not an easy task because species and community succession are interlinked with environmental stressors, our results call for a deeper exploration of the ecophysiological drivers of isoprene biosynthesis by phytoplankton. As a matter of fact, whilst isoprene production is *grosso modo* related to phytoplankton biomass and primary production (Fig. 4), the resulting isoprene concentration does not necessarily follow indicators of phytoplankton biomass such as chl *a* but it is further influenced by environmental factors such as SST^{12–14,51}. In spite of the lack of a mechanistic explanation, we conclude that temperature plays an important role in governing chl *a*-normalised isoprene production across regions of the open ocean. While expanding the lab-derived database of specific isoprene production rates across phytoplankton taxa is always desirable, we argue there is a need for in situ measurements under variable natural conditions if we are to reliably predict isoprene production in the ocean.

We also show that the loss terms in the cycle are more complex and variable than believed, with a microbiota-dependent sink that is tightly coupled to production and can dominate over ventilation in chl *a*-rich waters (Fig. 4). Considering all sinks together (ventilation, biological and chemical loss and, on one occasion, vertical mixing), the resulting total turnover times of isoprene in the surface mixed layer of the open ocean are in the order of one or two weeks in oligotrophic waters but can be as short as 1 to 4 days in productive waters. The microorganisms and metabolic mechanisms involved in isoprene biological consumption³⁴ warrant further investigation because this important sink will be regulated by triggers of microbial speciation and activity, potential co-metabolisms, and microbial mortality by predators and viruses. Our results also indicate that chemical consumption is more variable than estimated hitherto and has abiotic and biotic terms involving photochemically as well as biologically derived oxidants. All in all, isoprene concentration and emission to the atmosphere can no longer be regarded as controlled only by phytoplankton biomass and functional types, with fixed loss rates dominated by the physicochemical processes (air–sea exchange and oxidation), but rather intimately connected to the variable structure and dynamics of the pelagic microbial food web.

Methods

Sampling and physical measurements. Mediterranean coastal water samples were collected in March and May 2021 at the Blanes Bay Microbial Observatory site⁵², over a 20 m water column, and in August 2021 at a rocky pier of the Barceloneta beach (Barcelona), at 20 cm from patches of the seaweeds *Dictyoma dichotoma* and *Corallina elongata*. Surface (0.2 m) seawater was hand-collected from a boat or the rocks, and the temperature was recorded with a calibrated SAIVA/S SD204 CTD sensor. Samples were kept in the dark and taken to the ICM-CSIC lab within 3 h for incubations. The BIOGAPS-Moorea expedition took place in April 2018 at the northern coast of the island of Moorea, French Polynesia. Surface (0.2 m) seawater was hand-collected from a boat at two locations: in very shallow waters of the coastal coral reef lagoon, and 3.5 km offshore over a water column depth of 1100 m. Seawater temperature was recorded with an SBE56 sensor (Sea-Bird Sci.) continuously flushed with pumped-in surface seawater. Samples were taken to the Gump Research Station (University California Berkeley) on the island for processing. The HOTMIX cruise⁵³ traversed the Mediterranean Sea from East to West between 27 April and 29 May 2014 on board the R/V Sarmiento de

Gamboa. Seawater was collected with a General Oceanics rosette, equipped with 24 L Niskin bottles. Temperature and salinity were recorded with an SBE911 + CTD system (Sea-Bird Sci.). The TransPEGASO cruise⁴⁰ crossed the Atlantic Ocean from North to South on the R/V Hesperides, between 20 October and 21 November 2014. Surface seawater was sampled using the ship's underway pumping system, which had the water intake located 4–5 m below sea level. All the parts of the centrifugal pump (BKMKC-10.11, Tecnum) that were in contact with the fluid were made of polypropylene and glass. Seawater temperature and salinity were recorded continuously via the flow-through thermosalinograph SBE21 SeaCAT (Sea-Bird Sci.). The PEGASO cruise³⁹ was conducted on board de R/V Hesperides in the regions of Antarctic Peninsula, South Orkney and South Georgia Islands from 2 January to 11 February 2015. Seawater samples were collected from either the underway pumping system intake (same as above) or the uppermost (4 m) bottle of the rosette on SBE911 + CTD casts, which recorded temperature and salinity. In PEGASO, Lagrangian tracking of the surface (15 m) water patch was conducted using WOCE (World Ocean Circulation Experiment) standard drifters provided with an Iridium communication system. Each drifter consisted of a spherical floatable enclosure that contained a GPS and an emitter, from which 10 m cylindrical drogues hung 5 m below the sphere. The drifters sent their position every 30 min, and all ship operations were conducted next to them⁵⁴. The same Lagrangian approach was used to check for steady-state behaviour over 24 h in the open NW Mediterranean Sea during the BIOGAPS-MED cruise on board the R/V García del Cid on 20–21/06/2019 (Supplementary Fig. 2).

Incubation experiments. For loss kinetics experiments with coastal water (Fig. 1a and Supplementary Table 1), duplicate all-glass bottles (2 L) were filled, leaving no headspace, and incubated in the dark in a water bath kept at the in situ temperature ± 0.5 °C. Aliquots for duplicate isoprene analysis were taken from both bottles at t_0 and 2–4 further time points, never removing more than 15% of the bottle volume in total. Since opening the bottles caused the loss of the headspace, at each time point isoprene concentrations were corrected for this loss using the volumetric headspace:water ratio and the dependence of the isoprene Henry's law constant on temperature⁵⁵:

$$d(\text{LN}(H^{cp}))/d(1/T) = 4400$$

$$H^{cc} = [\text{iso}_a]/[\text{iso}_w] = RT \times H^{cp}$$

where H^{cp} is the Henry solubility, T is the incubation temperature in Kelvin, H^{cc} is the dimensionless Henry solubility, $[\text{iso}_a]$ and $[\text{iso}_w]$ are the isoprene concentrations in air (headspace) and water, respectively, and R is the gas constant.

For the chemical oxidation assay (Fig. 1b and Supplementary Table 1), coastal water was filtered sequentially through polycarbonate 3 and 0.2 μm pore-size filters, and the filtrate was used to fill four series of four gas-tight glass 30 mL vials. A working bromoperoxidase (BrPO) solution was prepared by dissolving 10 units of *Corallina officinalis* BrPO (Merck) with 100 μl of HEPES (4-(2-hydroxyethyl)-1-piperazineethanesulfonic acid) buffer 0.1 mol L⁻¹ in 900 μl of MilliQ water. One of the series of vials had only filtered water, another was added 10 μmol L⁻¹ of H₂O₂ (Merck), another was added BrPO to a final concentration of 0.0025 units mL⁻¹, and another was added both H₂O₂ and BrPO. Together with a series of non-filtered water, they were all incubated in the dark in a water bath kept at the in situ temperature (24 ± 0.5 °C). The initial isoprene concentration was measured from the filtrate before filling the vials, and t_1 , t_2 , t_3 , and t_4 concentrations were measured each sacrificing one of the vials.

For the 11 offshore experiments (Fig. 3, Supplementary Fig. 1 and Supplementary Table 2), duplicate all-glass bottles (0.5 L) were filled, leaving no headspace. One of the bottles was analysed in duplicate for isoprene to set the initial concentration. The other bottle was not opened and dark-incubated for 24 h in a tank with constant flushing of pumped-in surface ocean water, to keep incubation temperature the same as in situ. At the conclusion of the incubation time, isoprene concentration was analysed in sequential duplicates, each with its exact incubation time. The sample PEGASO B3 was incubated for only 9 h. The loss rate constant of isoprene k_{loss} (d⁻¹) was calculated as the slope of the natural logarithm of the concentration vs. time, under two assumptions: (a) consumption follows first-order kinetics, as in the case of other trace gases such as dimethyl sulfide⁵⁶ and methyl halides⁵⁷; coastal water experiments showed that first-order was a better approximation than zero-order (linear) kinetics (Fig. 1a and Supplementary Table 1); (b) isoprene production by phytoplankton, which is linked to photosynthesis²⁵, is mostly arrested over the 24 h of incubation in the dark; if biosynthesis resumed for a while in the dark³³, this would have reduced apparent loss and would have caused underestimation of k_{loss} . The error of k_{loss} was the standard error of the slope of Ln(concentration) vs. time.

Isoprene concentration. Isoprene was measured along with other volatile compounds on a gas chromatography–mass spectrometry system (5975-T LTM GC/MS, Agilent Technologies). Aliquots of 25 mL were drawn from the glass bottle with a glass syringe with a Teflon tube and filtered through a 25 mm glass fibre filter while introduced into a purge and trap system (Stratum, Tekmar Teledyne). The sample was purged by bubbling with 40 mL min⁻¹ of ultrapure He for 12 min while heated to 30 °C. The stripped volatiles were trapped on solid adsorbent (VOCARB 3000) at room temperature and thermally desorbed (250 °C) into the

GC. Isoprene monitored as m/z 67 in selected ion monitoring mode, had a retention time of 2.4 min in the LTM DB-VRX chromatographic column held at 35 °C. The detection limit was 1 pmol L⁻¹, and the analytical precision was 5%. In HOTMIX, TransPEGASO and PEGASO, calibration was performed by injections of a gaseous mixture of isoprene in N₂. In BIOGAPS-Moorea and coastal water experiments, a liquid standard solution prepared in cold methanol and subsequently diluted in MilliQ water was used instead.

Isoprene ventilation rate constant. The isoprene ventilation or air–sea exchange fluxes (F_{vent} , in nmol m⁻² d⁻¹) were calculated as:

$$F_{\text{vent}} = k_{\text{AS}} \times ([\text{iso}_w] - [\text{iso}_a]/K_{\text{H}}) \approx k_{\text{AS}} \times [\text{iso}_w]$$

where $[\text{iso}_w]$ is the isoprene concentration in surface seawater, $[\text{iso}_a]$ is the isoprene concentration in the air, K_{H} is Henry's Law constant for isoprene, and k_{AS} is the gas exchange velocity (cm h⁻¹). Air-side isoprene can be considered near zero and neglected for flux calculations because isoprene is highly reactive in the atmosphere, and it is largely supersaturated in the surface ocean. k_{AS} was estimated using⁵⁸:

$$k_{\text{AS}} = 0.251 \times U_{10}^2 \times (\text{Sc}/660)^{-0.5}$$

where U_{10} is the wind speed at 10 m (m s⁻¹), and Sc is the Schmidt number (non-dimensional). On cruises, the wind speed was measured by the ships' meteorological stations and averaged over a period of 24 h, which was the duration of the incubations. In offshore Mo'orea, we recorded wind speed on the boat with a portable Skywatch BL500 micrometeorological station. This instantaneous wind speed was converted to the daily average by applying the factor between instantaneous and daily average wind speeds measured at the Gump Station onshore. Sc was computed¹⁸ as:

$$\text{Sc} = 3913.15 + 162.13 \times \text{SST} + 2.67 \times \text{SST}^2 + 0.012 \times \text{SST}^3$$

where SST is in degrees Celsius (°C). The error of the computed ventilation fluxes is estimated⁵⁸ to be 20%. To convert the flux F_{vent} (nmol m⁻² d⁻¹) into the ventilation rate constant k_{vent} (d⁻¹), the flux was divided by the mixed layer depth (Z_{ML} , m) and by the isoprene concentration (nmol m⁻³), assuming that the surface concentration was equal to the average concentration in the mixed layer¹⁴. During HOTMIX and PEGASO, Z_{ML} was determined from CTD profiles as the depth at which density was 0.125 kg m⁻³ higher than that at 5 m. In the case of the TransPEGASO cruise and the BIOGAPS-Moorea expedition, where no CTD casts were conducted, we used the geolocalised monthly values from a global climatology⁵⁹.

Isoprene vertical mixing rate constant. In the case of the three PEGASO samples (sampling sites #9–11), k_{mix} was estimated from measured vertical profiles of isoprene concentration and the turbulent diffusion across the pycnocline (K_z). Thus, the vertical mixing flux at the bottom of the ML (F_{mix} , nmol m⁻² d⁻¹) was calculated as:

$$F_{\text{mix}} = K_z \times (\Delta[\text{iso}]/\Delta z)$$

where a $K_z = 2.6 \text{ m}^2 \text{ d}^{-1}$ (or $0.3 \text{ cm}^2 \text{ s}^{-1}$) was considered appropriate yet conservative for the Southern Ocean⁶⁰. $\Delta[\text{iso}]$ (nmol m⁻³) was the isoprene concentration gradient across the upper pycnocline, and Δz (m) was the distance covered by this gradient. Depending on the location of the concentration maximum, F_{mix} was positive (loss term, export from the ML) or negative (gain term, import into the ML). k_{mix} (d⁻¹) was calculated by dividing F_{mix} by the surface isoprene concentration and Z_{ML} (determined from the CTD profiles as above). We note that using a wider range of K_z for Southern Ocean locations^{61,62} (0.1–1.0 cm² s⁻¹) would give 0.3–3 times the estimates of the k_{mix} at sampling sites #9–11; however, the contribution of k_{mix} to the calculation of k_{prod} is so small (compared to those of the other sinks) that the effect of the K_z range on k_{prod} was only noticeable in #11 ($\pm 8\%$ of k_{prod}). For HOTMIX, TransPEGASO and BIOGAPS-Moorea, k_{mix} could not be estimated from in situ data and a fixed value of -0.005 d^{-1} was taken from the global integral suggested by a model¹⁷.

Chlorophyll a concentration. Seawater 250-mL samples were filtered on glass fibre filters, which were extracted with 90% acetone at 4 °C in the dark for 24 h. The fluorescence of extracts was measured with a calibrated Turner Designs fluorometer.

Bacterial abundance. Aliquots of 2 mL of the initial sample were fixed with 1% paraformaldehyde plus 0.05% glutaraldehyde and stored frozen at -80 °C . The numbers of heterotrophic bacteria were determined by flow cytometry (Cube 8, Partec) after staining with SYBR-Green⁶³.

Data availability

All data needed to evaluate the conclusions are available in <https://doi.org/10.5281/zenodo.5794234>.

Received: 4 October 2021; Accepted: 18 January 2022;

Published online: 08 February 2022

References

- Guenther, A. B. et al. The model of emissions of gases and aerosols from nature version 2.1 (MEGAN2.1): an extended and updated framework for modeling biogenic emissions. *Geosci. Model Dev.* **5**, 1471–1492 (2012).
- Saunio, M. et al. The global methane budget 2000–2012. *Earth Syst. Sci. Data* **8**, 697–751 (2016).
- Medeiros, D., Blitz, M., James, L., Speak, T. & Seakins, P. Kinetics of the reaction of OH with isoprene over a wide range of temperature and pressure including direct observation of equilibrium with the OH adducts. *J. Phys. Chem. A* **122**, 7239–7255 (2018).
- Claeys, M. et al. Formation of secondary organic aerosols through photooxidation of isoprene. *Science* **303**, 1173–1176 (2004).
- Hu, Q.-H. et al. Secondary organic aerosols over oceans via oxidation of isoprene and monoterpenes from Arctic to Antarctic. *Sci. Rep.* **3**, 2280 (2013).
- Carlsaw, K. et al. Large contribution of natural aerosols to uncertainty in indirect forcing. *Nature* **503**, 67–71 (2013).
- Pacifico, F., Harrison, S., Jones, C. & Sitch, S. Isoprene emissions and climate. *Atmos. Environ.* **43**, 6121–6135 (2009).
- Bonsang, B., Polle, C. & Lambert, G. Evidence for marine production of isoprene. *Geophys. Res. Lett.* **19**, 1129–1132 (1992).
- Broadgate, W. G., Malin, G., Kupper, F. C., Thompson, A. & Liss, P. S. Isoprene and other non-methane hydrocarbons from seaweeds: a source of reactive hydrocarbons to the atmosphere. *Mar. Chem.* **88**, 61–73 (2004).
- Loreto, F. & Schnitzler, J.-P. Abiotic stresses and induced BVOCs. *Trends Plant Sci.* **15**, 154–166 (2010).
- McGenity, T. J., Crombie, A. T. & Murrell, J. C. Microbial cycling of isoprene, the most abundantly produced biological volatile organic compound on Earth. *The ISME J.* **12**, 931–941 (2018).
- Dani, K. G. S. & Loreto, F. Trade-off between dimethyl sulfide and isoprene emissions from marine phytoplankton. *Trends Plant Sci.* **22**, 361–372 (2017).
- Ooki, A., Nomura, D., Nishino, S., Kikuchi, T. & Yokouchi, Y. A global scale map of isoprene and volatile organic iodine in surface seawater of the Arctic, Northwest Pacific, Indian, and Southern Oceans. *J. Geophys. Res.* **120**, 4108–4128 (2015).
- Hackenberg, S. C. et al. Potential controls of isoprene in the surface ocean. *Global Biogeochem. Cycles* **31**, 644–662 (2017).
- Ciuraru, R. et al. Unravelling new processes at interfaces: photochemical isoprene production at the sea surface. *Environ. Sci. Technol.* **49**, 13199–13205 (2015).
- Brüggenmann, M., Hayeck, N. & George, C. Interfacial photochemistry at the ocean surface is a global source of organic vapors and aerosols. *Nat. Comm.* **9**, 2101 (2018).
- Conte, L., Szopa, S., Aumont, O., Gros, V. & Bopp, L. Sources and sinks of isoprene in the global open ocean: simulated patterns and emissions to the atmosphere. *J. Geophys. Res.* **125**, e2019JC015946 (2020).
- Palmer, P. I. & Shaw, S. L. Quantifying global marine isoprene fluxes using MODIS chlorophyll observations. *Geophys. Res. Lett.* **32**, L09805 (2005).
- Huang, D., Zhang, X., Chen, Z. M., Zhao, Y. & Shen, X. L. The kinetics and mechanism of an aqueous phase isoprene reaction with hydroxyl radical. *Atmos. Chem. Phys.* **11**, 7399–7415 (2011).
- Acuña Alvarez, L., Exton, D. A., Suggett, D. J., Timmis, K. N. & McGenity, T. J. Characterization of marine isoprene-degrading communities. *Environ. Microbiol.* **11**, 3280–3291 (2009).
- Johnston, A. et al. Identification and characterisation of isoprene-degrading bacteria in an estuarine environment. *Environ. Microbiol.* **19**, 3526–3537 (2017).
- Moore, R. M. & Wang, L. The influence of iron fertilization on the fluxes of methyl halides and isoprene from ocean to atmosphere in the SERIES experiment. *Deep Sea Res. Part II* **53**, 2398–2409 (2006).
- Booge, D. et al. Marine isoprene production and consumption in the mixed layer of the surface ocean – a field study over two oceanic regions. *Biogeosciences* **15**, 649–667 (2018).
- Moore, E. R., Weaver, A. J., Davis, E. W., Giovannoni, S. J. & Halsey, K. H. Metabolism of key atmospheric volatile organic compounds by the marine heterotrophic bacterium *Pelagibacter* HTCC1062 (SAR11). *Environ. Microbiol.* <https://doi.org/10.1111/1462-2920.15837> (2021).
- Bonsang, B. et al. Isoprene emission from phytoplankton monocultures: the relationship with chlorophyll-a, cell volume and carbon content. *Environ. Chem.* **7**, 554–563 (2010).
- Claeys, M. et al. Formation of secondary organic aerosols from isoprene and its gas-phase oxidation products through reaction with hydrogen peroxide. *Atmos. Environ.* **38**, 4093–4098 (2004).
- Lin, C. Y. & Manley, S. L. Bromoform production from seawater treated with bromoperoxidase. *Limnol. Oceanogr.* **57**, 1857–1866 (2012).
- Vitler, H. Peroxidases from phaeophyceae. IV. Fractionation and localization of peroxidase isoenzymes. *Botanica Marina* **26**, 451–455 (1983).

29. Müller, E., von Gunten, U., Bouchet, S., Droz, B. & Winkel, L. H. E. Reaction of DMS and HOBr as a sink for marine DMS and an inhibitor of bromoform formation. *Environ. Sci. Technol.* **55**, 5547–5558 (2021).
30. Zinser, E. R. The microbial contribution to reactive oxygen species dynamics in marine ecosystems. *Environ. Microbiol. Rep.* **10**, 412–427 (2018).
31. Milne, A., Davey, M. S., Worsfold, P. J., Achterberg, E. P. & Taylor, A. R. Real-time detection of reactive oxygen species generation by marine phytoplankton using flow injection-chemiluminescence. *Limnol. Oceanogr. Methods* **7**, 706–715 (2005).
32. Rusak, S. A., Peake, B. M., Richard, L. E., Nodder, S. D. & Cooper, W. J. Distributions of hydrogen peroxide and superoxide in seawater east of New Zealand. *Mar. Chem.* **127**, 155–169 (2011).
33. Ooki, A. et al. Isoprene production in seawater of Funka Bay, Hokkaido, Japan. *J. Oceanogr.* <https://doi.org/10.1007/s10872-019-00517-6> (2019).
34. Dawson, R. A. et al. The microbiology of isoprene cycling in aquatic ecosystems. *Aquat. Microb. Ecol.* **87**, 79–98 (2021).
35. Moore, E. R., Davie-Martin, C. L., Giovannoni, S. J. & Halsey, K. H. *Pelagibacter* metabolism of diatom-derived volatile organic compounds imposes an energetic tax on photosynthetic carbon fixation. *Environ. Microbiol.* **22**, 1720–1733 (2020).
36. Gasol, J. M. & Duarte, C. M. Comparative analyses in aquatic microbial ecology: how far do they go? *FEMS Microbiol. Ecol.* **31**, 99–106 (2000).
37. Sinha, V. et al. Air-sea fluxes of methanol, acetone, acetaldehyde, isoprene and DMS from a Norwegian fjord following a phytoplankton bloom in a mesocosm experiment. *Atmos. Chem. Phys.* **7**, 739–755 (2007).
38. Johnson, T. L., Palenik, B. & Brahamsh, B. Characterization of a functional vanadium-dependent bromoperoxidase in the marine cyanobacterium *Synechococcus* sp. cc93111. *J. Phycol.* **47**, 792–801 (2011).
39. Zamanillo, M. et al. Distribution of transparent exopolymer particles (TEP) in distinct regions of the Southern Ocean. *Sci. Total Environ.* **691**, 736–748 (2019).
40. Zamanillo, M. et al. Main drivers of transparent exopolymer particle distribution across the surface Atlantic Ocean. *Biogeosciences* **16**, 733–749 (2019).
41. Booge, D. et al. Can simple models predict large-scale surface ocean isoprene concentrations? *Atmos. Chem. Phys.* **16**, 11807–11821 (2016).
42. Morel, A. et al. Examining the consistency of products derived from various ocean color sensors in open ocean (Case 1) waters in the perspective of a multi-sensor approach. *Rem. Sens. Environ.* **111**, 69–88 (2007).
43. Galí, M., Devred, E., Levasseur, M., Royer, S. J. & Babin, M. A remote sensing algorithm for planktonic dimethylsulfoniopropionate (DMSP) and an analysis of global patterns. *Rem. Sens. Environ.* **171**, 171–184 (2015).
44. Davie-Martin, C. L., Giovannoni, S. J., Behrenfeld, M. J., Penta, W. B. & Halsey, K. H. Seasonal and spatial variability in the biogenic production and consumption of volatile organic compounds (VOCs) by marine plankton in the North Atlantic Ocean. *Front. Mar. Sci.* **7**, 611870 (2020).
45. Meskhidze, N., Sabolis, A., Reed, R. & Kamykowski, D. Quantifying environmental stress-induced emissions of algal isoprene and monoterpenes using laboratory measurements. *Biogeosciences* **12**, 637–651 (2015).
46. Fall, R. & Copley, S. D. Bacterial sources and sinks of isoprene, a reactive atmospheric hydrocarbon. *Environ. Microbiol.* **2**, 123–130 (2000).
47. Shaw, S. L., Chisholm, S. W. & Prinn, R. G. Isoprene production by *Prochlorococcus*, a marine cyanobacterium, and other phytoplankton. *Mar. Chem.* **80**, 227–245 (2003).
48. Gantt, B., Meskhidze, N. & Kamykowski, D. A new physically-based quantification of isoprene and primary organic aerosol emissions from the world's oceans. *Atmos. Chem. Phys.* **9**, 4915–4927 (2009).
49. Exton, D. A., Suggett, D. J., McGenity, T. J. & Steinke, M. Chlorophyll-normalized isoprene production in laboratory cultures of marine microalgae and implications for global models. *Limnol. Oceanogr.* **58**, 1301–1311 (2013).
50. Shaw, S. L., Gantt, B. & Meskhidze, N. Production and emissions of marine isoprene and monoterpenes: a review. *Adv. Meteorol.* **2010**, 408696 (2010).
51. Rodríguez-Ros, P. et al. Distribution and drivers of marine isoprene concentration across the Southern Ocean. *Atmosphere* **11**, 556 (2020).
52. Gasol, J. M. et al. Seasonal patterns in phytoplankton photosynthetic parameters and primary production at a coastal NW Mediterranean site. *Sci. Mar.* **80S1**, 63–77 (2016).
53. Benavides, M. et al. Basin-wide N₂ fixation in the deep waters of the Mediterranean Sea. *Global Biogeochem. Cycles* **30**, 952–961 (2016).
54. Royer, S.-J. et al. A high-resolution time-depth view of dimethylsulfide cycling in the surface sea. *Sci. Rep.* **6**, 32325 (2016).
55. Sander, R. Compilation of Henry's law constants (version 4.0) for water as solvent. *Atmos. Chem. Phys.* **15**, 4399–4981 (2015).
56. Toole, D. A., Slezak, D., Kiene, R. P., Kieber, D. J. & Siegel, D. A. Effects of solar radiation on dimethylsulfide cycling in the western Atlantic Ocean. *Deep Sea Res. Part I* **53**, 136–153 (2006).
57. Tokarczyk, R., Goodwin, K. D. & Saltzman, E. S. Methyl chloride and methyl bromide degradation in the Southern Ocean. *Geophys. Res. Lett.* **30**, 1808 (2003).
58. Wanninkhof, R. Relationship between wind speed and gas exchange over the ocean revisited. *Limnol. Oceanogr. Methods* **12**, 351–362 (2014).
59. Holte, J., Talley, L. D., Gilson, J. & Roemmich, D. An Argo mixed layer climatology and database. *Geophys. Res. Lett.* **44**, 5618–5626 (2017).
60. Yang, M. et al. Lagrangian evolution of DMS during the Southern Ocean gas exchange experiment: the effects of vertical mixing and biological community shift. *J. Geophys. Res.* **118**, 6774–6790 (2013).
61. Cisewskia, B., Strassa, V. H. & Prandke, H. Upper-ocean vertical mixing in the Antarctic Polar Front Zone. *Deep Sea Res. II* **52**, 1087–1108 (2005).
62. Law, C. S., Abraham, E. R., Watson, A. J. & Liddicoat, M. I. Vertical eddy diffusion and nutrient supply to the surface mixed layer of the Antarctic circumpolar current. *J. Geophys. Res.* **108**, 3272 (2003).
63. Gasol, J. M. & del Giorgio, P. A. Using flow cytometry for counting natural planktonic bacteria and understanding the structure of planktonic bacterial communities. *Sci. Mar.* **64**, 197–224 (2000).

Acknowledgements

We are thankful to colleagues who provided chlorophyll and bacterial data: J.M. Gasol and J. Aristegui (HOTMIX), S. Nunes, M. Estrada and M.M. Sala (PEGASO and TransPEGASO), and C. Marrasé and M. Cabrera (Mo'orea). We are grateful to the crews and technicians on board the R/Vs Sarmiento de Gamboa and Hesperides, and to the managers and staff of the Gump Station in Mo'orea (administered by UC Berkeley). This research was supported by the Spanish national funding plan for science through projects PEGASO (CTM2012-37615) and BIOGAPS (CTM2016-81008-R) to RS, and through the 'Severo Ochoa Centre of Excellence' accreditation (CEX2019-000928-S) to the ICM-CSIC. PC-G and MM-N were supported by FPI Ph.D. fellowships from the Spanish national funding plan for science, while PR-R was supported by a 'La Caixa' Foundation Ph.D. fellowship. RS is a holder of a European Research Council Advanced Grant (ERC-2018-ADG-834162) under the EU's Horizon H2020 research and innovation programme.

Author contributions

RS designed the work, ran some of the experiments and measurements, processed data, made figures and wrote the paper with contributions from co-authors. PC ran most of the open-ocean experiments and isoprene measurements. PR-R processed data and made some of the figures. MM-N ran the consumption kinetics and oxidation experiments with coastal waters and one of the open-ocean experiments and processed data.

Competing interests

The authors declare no competing interests.

Additional information

Supplementary information The online version contains supplementary material available at <https://doi.org/10.1038/s43247-022-00352-6>.

Correspondence and requests for materials should be addressed to Rafel Simó.

Peer review information *Communications Earth & Environment* thanks Atsushi Ooki and the other, anonymous, reviewers for their contribution to the peer review of this work. Primary Handling Editors: Clare Davis. Peer reviewer reports are available.

Reprints and permission information is available at <http://www.nature.com/reprints>

Publisher's note Springer Nature remains neutral with regard to jurisdictional claims in published maps and institutional affiliations.



Open Access This article is licensed under a Creative Commons Attribution 4.0 International License, which permits use, sharing, adaptation, distribution and reproduction in any medium or format, as long as you give appropriate credit to the original author(s) and the source, provide a link to the Creative Commons license, and indicate if changes were made. The images or other third party material in this article are included in the article's Creative Commons license, unless indicated otherwise in a credit line to the material. If material is not included in the article's Creative Commons license and your intended use is not permitted by statutory regulation or exceeds the permitted use, you will need to obtain permission directly from the copyright holder. To view a copy of this license, visit <http://creativecommons.org/licenses/by/4.0/>.

© The Author(s) 2022